Front. Environ. Sci. Eng. 2020, 14(1): 16
https://doi.org/10.1007/s11783-019-1195-3

RESEARCH ARTICLE

In situ formation of bimetallic FeNi nanoparticles on sand through green technology: Application for tetracycline removal

Ravikumar KVG [*], Debayan Ghosh [*], Mrudula Pulimi, Chandrasekaran Natarajan, Amitava Mukherjee (✉)

Centre for Nanobiotechnology, VIT, Vellore, Tamil Nadu, India

HIGHLIGHTS

- In situ preparation of FeNi nanoparticles on the sand via green synthesis approach.
- Removal of tetracycline using GS-FeNi in batch and column study.
- Both reductive degradation and sorption played crucial role the process.
- Reusability of GS-FeNi showed about 77.39±4.3% removal on 4th cycle.
- TC by-products after interaction showed less toxic as compared with TC.

GRAPHIC ABSTRACT

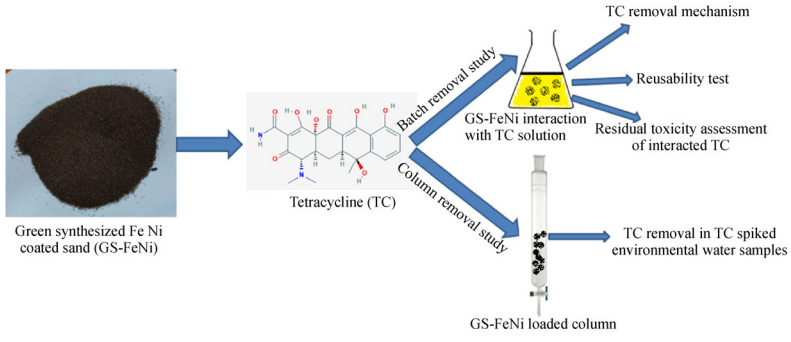

ARTICLE INFO

Article history:
Received 8 August 2019
Revised 14 October 2019
Accepted 21 October 2019
Available online 5 December 2019

Keywords:
GS-FeNi nanoparticles
Tetracycline removal
Re-usability
Residual toxicity
Column studies

ABSTRACT

In this study, FeNi nanoparticles were green synthesized using *Punica granatum* (pomegranate) peel extract, and these nanoparticles were also formed in situ over quartz sand (GS-FeNi) for removal of tetracycline (TC). Under the optimized operating conditions, (GS-FeNi concentration: 1.5% w/v; concentration of TC: 20 mg/L; interaction period: 180 min), 99±0.2% TC removal was achieved in the batch reactor. The removal capacity was 181±1 mg/g. A detailed characterization of the sorbent and the solution before and after the interaction revealed that the removal mechanism(s) involved both the sorption and degradation of TC. The reusability of reactant was assessed for four cycles of operation, and 77±4% of TC removal was obtained in the cycle. To judge the environmental sustainability of the process, residual toxicity assay of the interacted TC solution was performed with indicator bacteria (*Bacillus* and *Pseudomonas*) and algae (*Chlorella* sp.), which confirmed a substantial decrease in the toxicity. The continuous column studies were undertaken in the packed bed reactors using GS-FeNi. Employing the optimized conditions, quite high removal efficiency (978±5 mg/g) was obtained in the columns. The application of GS-FeNi for antibiotic removal was further evaluated in lake water, tap water, and ground water spiked with TC, and the removal capacity achieved was found to be 781±5, 712±5, and 687±3 mg/g, respectively. This work can pave the way for treatment of antibiotics and other pollutants in the reactors using novel green composites prepared from fruit wastes.

1 Introduction

Antibiotics are pharmaceutical compounds that play a crucial role in health, agriculture, and livestock industries. Conventionally, antibiotics are defined as those compounds, which suppress or hinder the growth of microorganisms on administration (Marzo and Dal Bo, 1998). They are assorted in the category of pharmaceutical and personal care products [PPCP]. However, over the last two decades, the increasing use of antibiotics has pre-eminently introduced various micro pollutants at various concentration levels in the aquatic environment (Gottschall et al., 2012).

Tetracycline (TC) is extensively used around the globe because of its lower production cost, ease of handling, and

✉ Corresponding author
E-mail: amit.mookerjea@gmail.com, amitav@vit.ac.in

[*]These authors contributed equally to this work.

its high effectiveness as a therapeutic (Kang et al., 2010). With escalated use, the quality of ground and surface water would be seriously affected as TCs have high solubility and long environmental half-life. Thus, continuing accumulation of TC in the aquatic environment poses an imminent threat to the environment (Miao et al., 2004). The consequences of tetracycline accumulation in fresh water environment and suggested that a substantial concentration of antibiotics is present in the aquatic environment (Danner et al., 2019). This makes the bacteria to become resistant in the environment, which is a potential threat to the ecosystem and animal health as it interferes with the aquatic food web by causing antibiotic pollution; thereby, other organisms are also greatly affected due to the toxicity of accumulated antibiotics (Danner et al., 2019). Tetracycline is hard to degrade as it gets converted into more potentially toxic substance over a prolonged period of time, and thus, contaminates various aquatic reservoirs resulting in chronic toxicity (Dai et al., 2019).

In recent years, nano zero valent iron (nZVI) is widely used for on-site treatment of organic and inorganic contaminants. It has been reported that nZVI particles are proven to be the most promising and efficient substances in the removal of various antibiotics from wastewater. The nZVI particles being strong, highly reactive, and possessing abundant reactive sites, are capable of eliminating various antibiotics from wastewater (Zhou et al., 2019). However, nZVI has few limitations (Dong et al., 2018a) like the passivation of active sites and diminished reactivity/efficiency due to the development of oxide layer on the nZVI surface. To overcome this, coupling of nZVI with a secondary metal has been attempted (Fowkes et al., 1970). Hence, bimetallic nanoparticles (BNPs) are increasingly applied for efficient remediation of contaminated wastewaters. Recently, MnO_2/graphene nanocomposite with excellent water solubility was prepared by hydrothermal method and was able to remove 99% of tetracycline efficiently from pharmaceutical wastewater after flocculation (Song et al., 2019). Oxytetracycline was efficiently removed from the aqueous solution by inert-metal-coated (Ni or Cu) nZVI particles, wherein the inert metal increases the electron transfer between the particles and can generate hydroxyl radicals, and thus, protect Fe^0 from getting oxidised (Wu et al., 2018). Wheat straw–supported nZVI composites were successfully used to remove chlortetracycline and copper ions through redox reaction and adsorption process in aqueous solution; thereby, providing new insights to the remediation of complex wastewater (Shao et al., 2020). Many researchers have shown that Fe-Ni is a suitable BNP for degradation of various therapeutics, such as tetracycline and doxorubicin (Kadu et al., 2017; Dong et al., 2018b). Fe-Cu BNPs has also been used for the efficient removal of oxytetracycline in the past (Wu et al., 2018). Fe/Cu-GO nanocomposite has been utilized for the effectual removal of tetracycline (Tabrizian et al., 2019). All these previous investigations employed various hazardous and toxic chemicals such as borohydride for the synthesis of nanoparticles, which may potentially increase the overall environmental toxicity. A plausible solution to this problem would be to biosynthesize the nanoparticles using the waste products (peels) of fruits, which possess the required bio-organics for the reaction. Numerous biologically active compounds are present in pomegranate, and hence, it has been used as a medicine for years. When compared to pomegranate seed and pulp, its extract has more antioxidant activity (Li et al., 2006). The peel extract has reducing ability due to its high polyphenolic content, which can be used for the synthesis of nanoparticles. In a previous report by Ahmad et al., pomegranate peel–mediated gold and silver nanoparticles were prepared (Ahmad et al., 2012). Hence, pomegranate peel extract was selected for the present study to synthesize FeNi nanoparticles. We recently reported a green synthetic process for preparing FeNi bimetallic nanoparticles using pomegranate peel extract (Ravikumar et al. 2019b).

However, agglomeration of nanoparticles often poses a serious problem and limits their use in large-scale reactor operations. Additionally, the direct use of FeNi nanoparticles in commercial application would be quite expensive. Thirdly, regeneration and reuse of the reactant is not possible if the bare nanoparticles are used for contaminant removal. To address these limitations an inert substrate or support system for the particles can be provided. Sand being an inert material provides effective support as the particles are formed as fine layers on the surface (Kango and Kumar, 2016). There were no prior studies on antibiotic removal using green-synthesized composite materials like bimetallic NPs coated on sand. The successful operation of such approaches can be scaled-up in column reactors for effective wastewater treatment.

The current study aims to couple the advantages of green-synthesized bimetallic nanoparticles with that of sand as an inert support material to develop (i) an environmentally sustainable composite material and (ii) a scalable process using these materials for treating pharmaceutical pollutants. After a detailed literature survey, the current investigation could be comprehended as one of the leading studies related to in situ green synthesis of FeNi nanoparticles on quartz sand (GS-FeNi) and their application as a sorbent in packed bed columns. GS-FeNi was synthesized using peel extracts of pomegranate and applied for TC removal in batch and column reactors. The mechanism of TC removal could be realized with the help of various analytical methods. The residual toxicity test of TC degraded compounds in the solution was also performed using indicator microorganisms such as bacteria (*Bacillus* and *Pseudomonas*) and algae (*Chlorella* sp.). The regeneration of the reactant materials was tested for up to four cycles of operation. The influence of parameters like flow rate, initial TC concentration, and

bed heights was analyzed in the TC removal process. GS-NiFe was tested in different water samples to validate its applicability in real conditions.

2 Materials and methods

2.1 Chemicals

Tetracycline TC (purity ⩾ 98%) was procured from Merck (Germany) (CAS Number: 60-54-8; λ_{max}: 360 nm), whereas nickel (II) sulfate ($NiSO_4$), ferric chloride ($FeCl_3$), and quartz sand (CAS Number 14808–60–7) were purchased from Sigma Aldrich. Glass wool was from Hi–Media Laboratories, Mumbai, India, and carboxymethyl cellulose (CMC) from Molychem, Mumbai, India. All the chemicals and reagents procured were ensured to be of analytical grade. Ultrapure deionized water (18.25 Ω) was utilized for solution preparation.

2.2 Green synthesis of Fe-Ni-NP–coated sand

Ethanolic extraction of pomegranate peel: After collecting pomegranates from a local vendor, the fruits were rinsed with tap water and manually peeled. The peels were dried in an oven at 60°C for 40 h, and the dry powder was extracted (15%) with 100% ethanol in a shaking incubator for 24 h. The mixtures were filtered through Whatman No.1 filter paper. Finally, the supernatant was collected and stored for further use at 20°C.

The green synthesis of Fe-Ni-NP–coated sand is schematically represented in Fig. S1 (Supplementary information). Pure and pristine quartz sand (100 g) was taken in a screw-capped bottle to which 150 mL of 0.1 M $FeCl_3$ solution was added slowly. The screw-capped bottle was then kept on an orbital shaker for 30 min for uniform mixing of $FeCl_3$ solution with sand. The sand coated with Fe was then dried overnight in a vacuum oven at 80°C. To the dried $FeCl_3$-coated sand, the ethanolic extract (10%) of pomegranate peel was introduced slowly at room temperature (29°C). The color of the mixture turned from golden yellow to black during the process. Following the addition of the entire pomegranate peel extract, the solution was kept on an orbital shaker for 30 min at room temperature for uniform mixing. CMC (0.1%) addition was carried out to stabilize NZVI. This mixture was kept on an orbital shaker for 1 h after adding 0.1 M $NiSO_4$ (150 mL) solution to it. Finally, the FeNi-coated sand was filtered through a Whatman No.1 filter paper before washing thrice with absolute ethanol and drying in a vacuum oven at 80°C.

2.3 Characterization of GS-FeNi

The synthesis of GS-FeNi was confirmed by X-Ray Diffraction (XRD) with CuK (λ = 1.5418 A°) radiation [Model: Advanced D8; Make: Bruker, Germany] to confirm the crystallinity of the synthesized bimetallic nanoparticles. Fourier transform-infrared spectrometry (FT-IR) [Model: IR Affinity-1; Make: Shimadzu, Japan] was employed to confirm the functional groups on the sorbent surface. The morphological investigations of the synthesized nanoparticles like particle shape and size analyses were performed with the help of Field-Emission Scanning Electron microscopy (FE-SEM) [Model: SUPRA 55; Make: Carl Zeiss, Germany]. The energy-dispersive spectroscopy (Oxford Inca EDS) attached to the FE-SEM was performed to analyze the elemental composition. Brunauer Emmett-Teller (BET) [Model: Tristar III; Make: Micromeritics, USA] was employed for the pore volume and surface area analyses.

2.4 Batch study of TC removal using GS-FeNi

The batch experiments for TC removal were conducted in a 250-mL conical flask by mixing 100 mL of TC solution with GS-FeNi. Various experimental parameters such as GS-FeNi weight (0.5%–1.5% w/v), interaction time (30–180 min), and initial concentration of TC (20–60 mg/L) were varied. All the tests were performed keeping temperature constant at 37°C and pH at 7 to simulate the natural conditions (Pulugandi, 2014; Arivoli et al., 2018). At definite time intervals, sample (2 mL) was collected from the screw-capped bottle and centrifuged (10 min) at 8000 rpm. After centrifugation, the sample was subjected to measurement of TC absorbance at 360 nm using a UV–visible spectrophotometer [Model: UV1750; Make: Shimadzu Corporation, Kyoto, Japan]. Removal (%) of TC was computed using Eq. (1) (Vijayakumar et al., 2013).

$$TC\ Removal(\%) = \frac{C_0 - C}{C_0} \times 100, \tag{1}$$

where, C_0 and C denote the TC initial and final concentrations (mg/L) at equilibrium.

2.5 Experimental data analysis using adsorption kinetics

The pseudo first order and second order models were fitted with the kinetics data. The equations were written as follows.

$$\ln\frac{q_e - q_t}{q_e} = -K_L t, \tag{2}$$

$$\frac{t}{q_t} = \frac{1}{2K' q^2 e} + \frac{t}{q_e}, \tag{3}$$

wherein K_L– removal rate constant of Lagergen (L/min); K'– adsorption rate constant of pseudo second order (mg/g); q_e and q_t are the amount of TC removed (mg/g) at equilibrium and time t, respectively. The linear relationship plots for pseudo first order [log (q_e–q_t) vs. t] and pseudo

second order [linear plot t/q_t vs. t] yield K_L and K', which can be calculated from the slope and intercept of the plot, respectively (Oladoja et al., 2009; Öztürk and Malkoc, 2014).

2.6 Adsorption isotherm

The equilibrium TC adsorption data at 27±1°C were modeled using Langmuir and Freundlich isotherms (Qiu et al., 2014) to study the mode of TC adsorption on GS-FeNi when the TC solution phase and GS-FeNi solid phase are in equilibrium.

The Langmuir adsorption isotherm is represented as:

$$\frac{C_e}{q_e} = \frac{1}{bq_{\max}} + \frac{C_e}{q_{\max}}, \quad (4)$$

wherein C_e is the equilibrium concentration of TC (mg/L) adsorbed by GS-FeNi; q_e is the amount of TC uptake (mg/g); $q_{\max}$ (mg/g) and b (L/mg) are Langmuir constants. The graph was plotted between C_e and C_e/q_e, to obtain values of $q_{\max}$ and b.

The Freundlich isotherm is represented by:

$$\log\ q_e = \log\ K_f + \frac{1}{n}\log\ C_e, \quad (5)$$

wherein C_e is the residual concentration of TC (mg/L) in solution; q_e is the amount of TC adsorbed on sorbent at equilibrium (mg/g). A graph was plotted between log q_e and log C_e to obtain values of K_f and n.

2.7 TC removal mechanism analysis

High-Resolution Liquid Chromatograph Mass Spectrometer (HRLC-MS) [Model: 1290 Infinity UHPLC System; Make: Agilent Technologies, USA) coupled with a PDA detector–mass spectrometer at a fixed wavelength (358 nm) was used to determine the products of TC that have been degraded by GS-FeNi upon interaction. Total Organic Carbon (TOC) in the solution was measured with the help of a TOC analyzer [Model: TOC-L; Make: Shimadzu] to determine whether degradation or adsorption has played a vital role in the mechanism of TC removal by GS-FeNi. The solution oxidation–reduction potential (ORP) was analyzed with a digital potentiometer (Model DP003, Pico, Chennai).

2.8 Reusability test

To assess the potential of TC removal by GS-FeNi for practical purposes, reusability test was done for up to four cycles. The interacted solution was collected from the batch reactor, and GS-FeNi was separated using centrifugation (6000 rpm, 10 min). The separated GS-FeNi was washed thoroughly with 0.05 mol/L of HCl solution, followed by a wash with de-ionized distilled water and kept inside a hot-air oven (80°C) for complete drying of the materials. The dried sand was then again used for TC removal under optimized conditions for the first cycle, and this procedure was repeated for the next three consecutive cycles in order to test the removal efficiency of the reused GS-FeNi. After the completion of four cycles of reusability test, the entire sand was reused for the synthesis of fresh GS-FeNi by washing the used sand with a mixture of concentrated HNO_3 and HCl in the ratio of 1:3, followed by a wash with deionized distilled water, and then, completely drying the sand in a hot-air oven at 100°C. The white crystalline quartz sand thus obtained can be used again without the need for procuring new sand every time (Huang et al., 2017; Weng et al., 2018).

After interaction, the supernatant was collected and centrifuged, filtered through 0.1-μm syringe filter, followed by 3-kDa filtration. Subsequently, the Fe and Ni ions released in the solution were estimated by AAS analysis.

For mass quantification of Fe and Ni formation on sand, 10 mg of GS-FeNi sand was acid digested in 10 mL of HNO_3 and diluted with milli-Q water and estimated by AAS analysis.

2.9 Residual toxicity assessment of interacted TC

Gram-positive bacterium (*Bacillus subtilis*), and Gram-negative (*Pseudomonas aeruginosa*), and freshwater microalga (*Chlorella* sp.) were selected as the test microorganism for cell viability assays of TC and GS-FeNi–treated TC. More details can be found in our previous publications (Natarajan et al., 2016; Roy et al., 2018; Ravikumar et al., 2019b).

2.10 Fixed-bed column study for TC removal

The fixed-bed column studies were executed in a continuous mode using a glass column (details of the set up are provided in our previous study, (Ravikumar et al., 2019b) with height: 30 cm and internal diameter: 2.5 cm packed with GS-FeNi. The tests were performed by varying the experimental parameters such as flow rates: 1–3 mL/min, influent concentration of TC: 20–60 mg/L, and bed heights: 3–10 cm. During the experimental period, 2.5 L of fresh solution containing TC was added to the inlet reservoir everyday only after confirming the concentration of TC by UV–visible spectrophotometry (UV1750, Shimadzu Corporation, Kyoto, Japan). A constant temperature of 30°C and pH 7 was maintained throughout the experiment. The columns were operated continuously without any break until the sorbent capacity of GS-FeNi was exhausted.

The TC content inside the column (W_{ad}) was calculated by multiplying the area below (or delimited by) the breakthrough curve (final TC concentration vs. time) with the flow rate. The total amount of TC passing into the column (W) was calculated by the equation. TC removal

percentage (%) and removal capacity (mg/g) can be determined by Eq. (6) and (7), respectively (Gokhale et al., 2009; Ravikumar et al., 2016a):

$$W = \frac{C_0 \times F \times t_e}{1000}, \quad (6)$$

wherein C_0 is the inlet TC concentration (mg/L), F indicates the flow rate (mL/min), t_e is the equilibrium time (min), and M is mass of the sorbent.

$$TC\ removal\ capacity(q) = \frac{W_{ad}}{M}. \quad (7)$$

2.11 TC removal in environmental water samples using column reactor

The water samples were collected from various sources such as household tap (Lat: 12°58′10.4″N, Long: 79°09′ 20.0″E), a recreational lake (Lat: 12°58′10.3″N, Long: 79°09′36.5″E) from places located in VIT campus, and a dug well (Lat: 12°57′55.5″N, Long: 79°09′15.5″) in Vaibhav Nagar, Katpadi, Vellore, Tamil Nadu. The optimum experimental conditions as obtained in the column tests were employed to test the TC removal capacity of GS-FeNi for water samples after spiking with specific concentrations of TC.

2.12 Statistical analysis

The entire set of tests was conducted in triplicates, and the data are presented as mean±standard error.

3 Results and discussion

3.1 Characterization studies of synthesized GS-FeNi

The FT-IR spectral analysis of GS-FeNi is given in Fig. S2 (supplementary information). The absence of Fe-O peak demonstrates the prominence of Fe^0 state in the synthesized particles (Ma et al., 2017). The peaks at 2334 cm^{-1}, 2157 cm^{-1}, and 1644 cm^{-1} appear due to the stretching vibrations of O-C-O and C = C functional groups, which strongly relate to the presence of polyphenols in the pomegranate peel extract (Kaviya, 2017). The results clearly indicate that the bio-organics from the fruit peel extract induced the formation of GS-FeNi on sand. This is also corroborated by the findings in our previous study on the synthesis of Fe-Ni particles using pomegranate peel extract (Ravikumar et al., 2019b).

The XRD spectral data for GS-FeNi [Fig. S3 (supplementary information)] indicate prominent diffraction peaks at 2θ = 45.78°, 50.01°, 53.54°, and 67.86° corresponding to crystal planes of (1 1 0), (2 0 0), (2 2 0), and (2 2 0), respectively [JCPDS file no. of Fe (52-0513) and Ni (04-0850)] (Du et al., 2017), which clearly signifies the formation of FeNi nanocomposite.

The SEM image of GS-FeNi is shown in Fig. S4 (supplementary information). The mean diameter of GS-FeNi was 161±43 nm, and the particles were mostly spherical. Further, EDX analysis of GS-FeNi confirmed the occurrence of both Fe and Ni in the ratio of 1:1 on the sand surface [Fig. S4 (supplementary information)].

The surface area of GS-FeNi (1.19 m^2/g) was observed to be increased as compared with sand alone (0.19 m^2/g). The pore volume of sand was-0.000309 cm^3/g, and after coating with nanoparticles, it was increased to 0.000356 cm^3/g. The detailed BET analysis results including N_2 adsorption/desorption, BET surface area, and BJH plot are given in Fig. S5 (supplementary information). The increase in GS-FeNi surface area and pore volume may be related to the coating of nanoparticles on the sand surface.

3.2 Effect of operating conditions

Previous reports suggest that various factors such as sorbent mass, time, and initial TC concentration play a crucial part in the sorbent reactivity toward the removal of dissolved TC in aqueous samples (Punamiya et al., 2015; Jin et al., 2018).

The GS-FeNi doses were varied by keeping other experimental parameters constant. As anticipated, with higher doses of GS-FeNi (1.5% w/v), the TC removal efficiency reached 99±0.2% within 180 min (Fig. 1A). At lower doses of 1% w/v and 0.5% w/v, the TC removal decreased to 85±0.7% and 76±0.3%, respectively. The findings were supported by previous reports on Cr(VI) removal using Fe nanoparticles (Jin et al., 2018) and magnetite nanoparticles-coated sand for As removal (Kango and Kumar, 2016).

The effects of increasing time period were assessed with initial dose of 1.5% w/v GS-FeNi, 20 mg/L TC concentration, and pH of 7 (Fig. 1B). After a duration of 180 min, no further increment in TC removal was observed. From these results, it can be concluded that the complete removal of TC using GS-FeNi required 180 min.

As the TC concentration was increased from 20 mg/L to 60 mg/L, a decline in the removal percentage of TC was obtained. The highest removal percentage was observed to be 99±0.2% at 20 mg/L of TC concentration, which decreased to 70±0.8% at 40 mg/L, and 59±0.4% at 60 mg/L of TC concentration (Fig. 1C), while the other experimental conditions were kept constant. These findings are in good agreement with earlier reports (Yue et al., 2009; Gheju et al., 2016). This correlates to the fact that there are only a limited number of reactive sites available for reaction for a given amount of GS-FeNi. Thus, with increase in initial concentration of TC, there was no additional increase in the number of reactive sites for the GS-FeNi, so the removal efficiency declined substantially.

Under optimum conditions (reaction time of 180 min; GS-FeNi weight of 1.5% w/v; influent TC concentration of

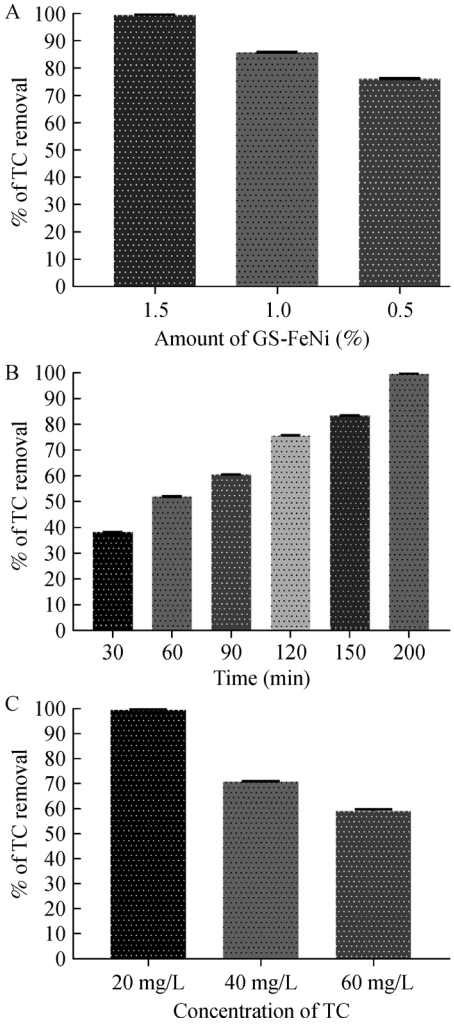

Fig. 1 Effect of various operating conditions during batch studies: (A) Effect of GS-FeNi load, (B) Effect of time, and (C) Effect of initial TC concentration.

20 mg/L), high removal efficiency of 99±0.2% was obtained. A control experiment was conducted with only Fe-coated sand, and only 67±0.6% removal was obtained under identical conditions. This demonstrates the effectiveness of nanocomposites in the removal of TC compared to pristine particles. From the previous reports, a comparison study of present sorbent with other sorbents was done (Table S1, Supplementary information). As compared to other available sorbents, the advantage of present study was economical process (green synthesis of FeNi), less dosage of nanocomposites was used without any irradiation. The removal efficiency of TC is relatively higher as compared to other methods.

3.3 Adsorption kinetics

The results were fitted to the common kinetic models represented (Table S2A, Supplementary information). A comparison of the correlation coefficients of the investigated models shows that pseudo second order (R^2 = 0.99) was most suitable to describe the adsorption process. The adsorption capacity (q_e) estimated from pseudo-second-order equation was in concurrence with the experimental values. The pseudo second order assumes that the adsorption process was chemisorptive in nature (Turku et al., 2007).

3.4 Adsorption isotherm

The adsorption isotherm data were recorded for three different initial concentrations of TC (20, 30, 40, 50, and 60 mg/L) for GS-FeNi at 180 min. The various isotherm parameters are tabulated in Table S2B (supplementary information). The best fit was obtained using the Langmuir model with a highest regression coefficient (r^2) of 0.99 and q_{max} of 123.43 mg/g. The theoretically quantified q_o from the Langmuir plot was close to the results obtained experimentally. These results suggest a monolayer sorption during the interaction (Tang et al., 2014; Xiong et al., 2018).

3.5 Mechanism(s) of TC removal

To ascertain the role of adsorption and degradation in the process, the variation of TOC during the interaction was studied and compared with the trend of TC removal. It is usually considered that if TC is only degraded into smaller compounds in the absence of adsorption, the TOC in the solution would remain constant throughout the test. However, as shown in Fig. 2A, the TOC declined during the reaction, confirming that adsorption had a key role to play. After 120 min, TOC reached equilibrium, while TC removal reached approximately only 70%. Therefore, it is inferred that both adsorption and degradation were involved in the removal process. This finding is also supported by previous reports on TC removal by chemically-synthesized FeNi BNP (Dong et al., 2018b).

As an electron donor, GS-FeNi was effective in creating a strong reducing environment in the solution. The values of oxidation–reduction potential (ORP) decreased from 370 to 187 mV during the reaction time (180 min) as can be seen in Fig. 2B, which corroborates the presence of reducing conditions during the interaction. The decline in oxidation–reduction potential (ORP) indicates the oxidation of GS-FeNi and consequent reduction of TC in the process.

The degradation products of TC were investigated using LC-MS analysis. The (m/z) ratio of 450 corresponding to the uninteracted TC has been established in our recent study (Ravikumar et al., 2019b). The LC-MS chromatograph (Fig. 3A) showed that the intensity of the main TC peak (450 m/z) decreased considerably after interaction with GS-FeNi, and additional peaks with m/z of 336, 240, and 118 emerged. The formed products at 336 (Berberine), 240 (1,2,8-Trihydroxyanthraquinone), and 118 (m-cresol)

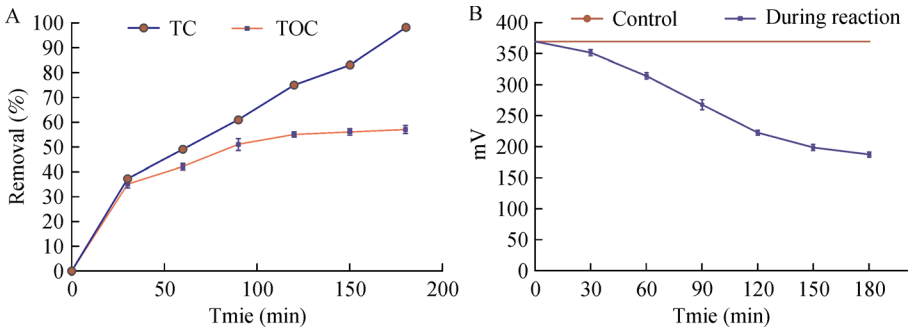

Fig. 2 (A) TC and TOC removal upon interaction of GS-FeNi with TC, (B) Changes in ORP during reaction.

m/z may be attributed to the carboatomic ring B break and benzene ring hydrogenation (Chen et al., 2017; Dong et al., 2018b; Jiang et al., 2018). The other products formed during the interaction, which had very low intensity, were not considered since those could be of transitional nature and only traces of them were present in the solution. Hence, with the supporting evidences from previous reports (Yan et al., 2016; Dong et al., 2018b), current results confirm that GS-FeNi was able to degrade TC into smaller organics. The degraded by-products are shown in Fig. 3B.

The changes in sorbent before and after interaction with TC was further confirmed through detailed characterization of the interacted solids using different analytical methods. The XRD patterns for GS-FeNi after interaction with TC are shown in Fig. 4. Peaks at 2θ: 45.78°, 50.01°, 53.54°, and 67.86° correspond to GS-FeNi. The appearance of iron oxide (Fe-O) peaks at 2θ: 36.76° and 59.5° corresponds to (3 1 1) and (6 1 1) crystal planes (Blowes et al., 1997), which proves the plausible GS-FeNi oxidation in the redox reaction throughout TC removal from the solution since these peaks were absent in the XRD patterns of uninteracted GS-FeNi as shown in Fig. S3 (supplementary information). It was also noted that there was a decline in the Fe^0 intensity and a new peak (Fe-O) appeared in the case of TC-interacted GS-FeNi, validating the possibility

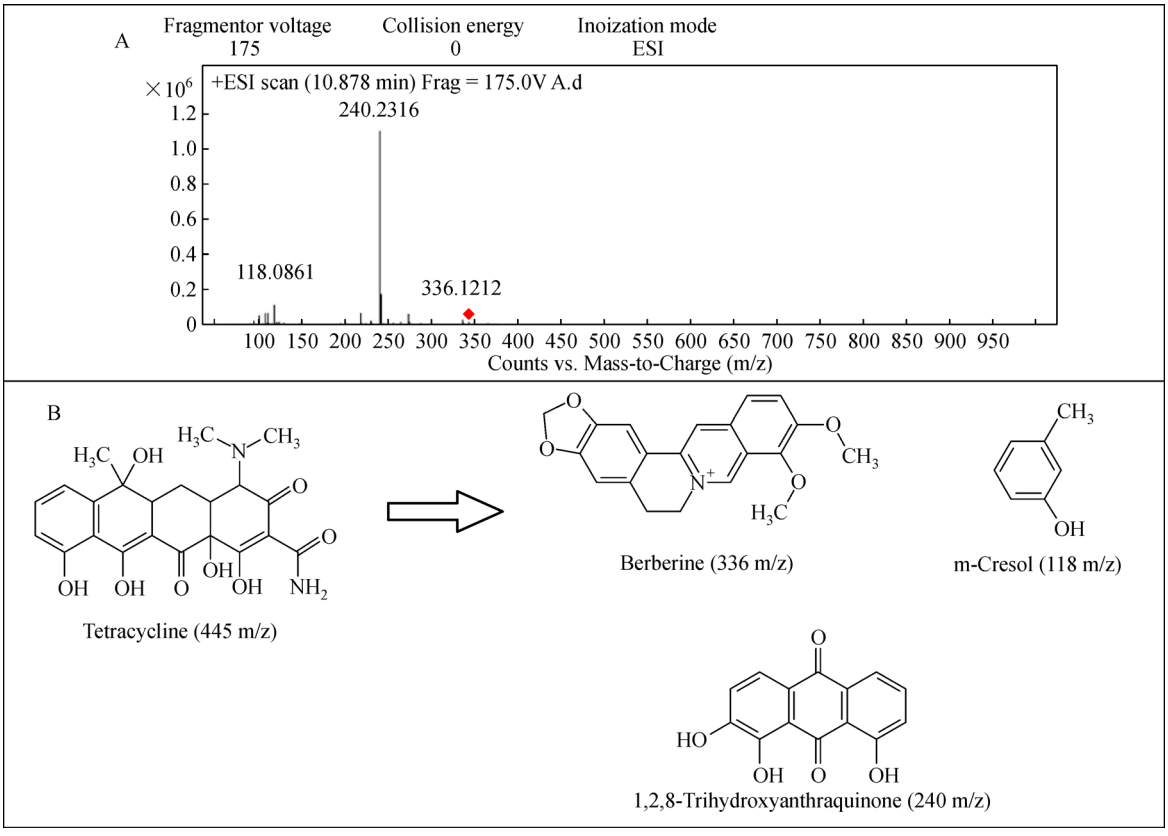

Fig. 3 (A) LC-MS result of GS-FeNi–interacted TC after 180 min of interaction, (B) proposed TC degradation pathways after reaction with GS-FeNi.

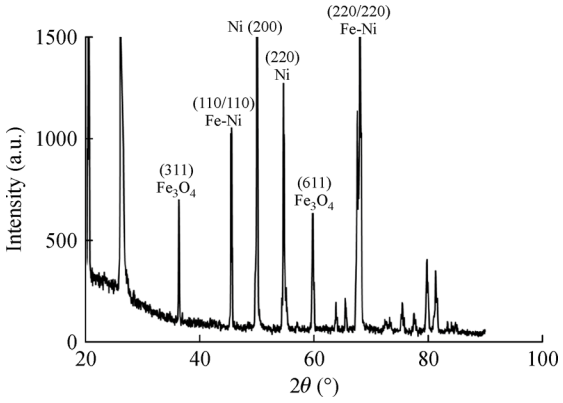

Fig. 4 XRD spectra of GS-FeNi after interaction with TC

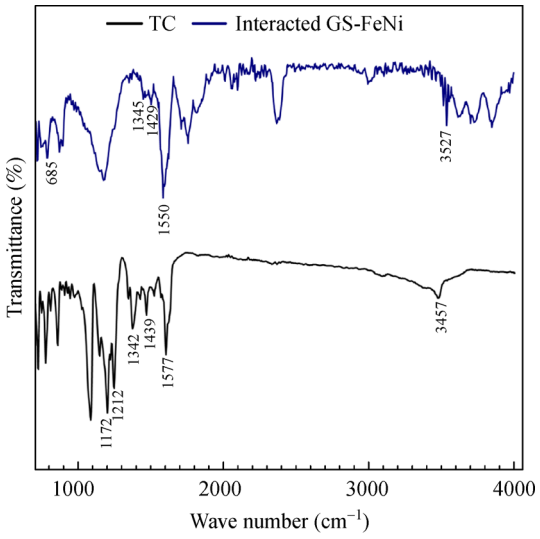

Fig. 5 FT-IR spectra of TC and TC-interacted GS-FeNi.

of a redox reaction between tetracycline and zero-valent Fe (Fu et al., 2013; Li et al., 2015).

The adsorption of tetracycline by GS-FeNi is supported by FT-IR spectral data (Fig. 5). The peaks at 3527, 1550, 1429, and 1345 cm^{-1} confirm the presence of adsorbed tetracycline on the surface of GS-FeNi. Also, the Fe-O peak at 685 cm^{-1} can be linked with possible surface oxidation of metallic zero-valent Fe.

The surface area of GS-FeNi was observed to decrease from 1.35 m^2/g to 1.19 m^2/g upon interaction with TC. The pore volume of un-interacted GS-FeNi was 0.000624 cm^3/g, and after interaction, it decreased to 0.000356 cm^3/g. The detailed BET analyses results, including N_2 adsorption/desorption, BET surface area, and BJH plot are given in Fig. S6 (supplementary information). The decline in GS-FeNi surface area and pore volume may be related to the adsorption of TC residues on the GS-FeNi surface.

From the above discussion, it can be concluded that TC was initially adsorbed on the GS-FeNi surface, and by the action of FeNi nanoparticles, TC was subsequently degraded into different smaller organics. The schematic representation of TC degradation is given in Fig. 6.

3.6 Residual toxicity of interacted TC

The cellular viability of the bacteria was considered to study the possible toxic effects of untreated TC and GS-FeNi–treated TC (Fig. 7A). Among the two strains, *Bacillus* sp. was more sensitive to the test substance tetracycline than *Pseudomonas* sp. The GS-FeNi–treated sample considerably enhanced the cell viability of the bacterial species as compared to that of untreated TC. The

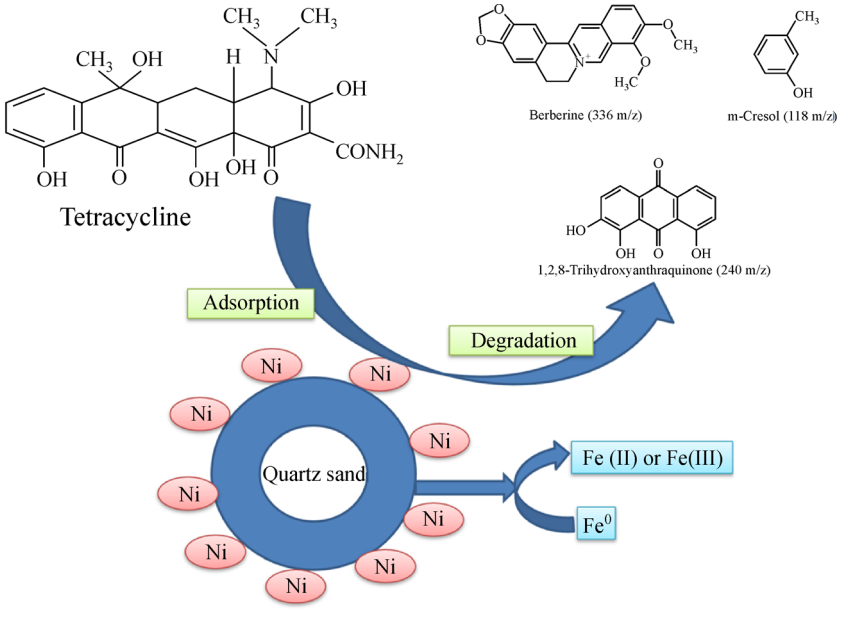

Fig. 6 Schematic representation of TC removal process.

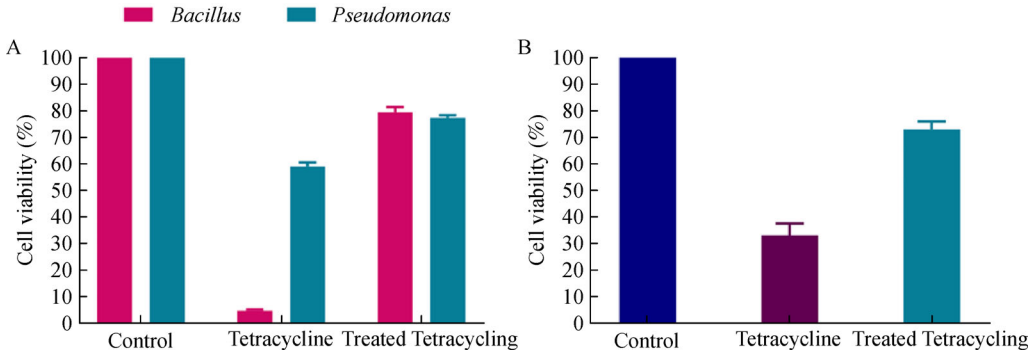

Fig. 7 Residual toxicity of degraded TC by-components toward (A) bacteria and (B) algae.

viability of algal cells upon treatment with untreated TC and GS-FeNi–treated TC is shown in Fig. 7B. Upon treatment with untreated TC, the viability of the cells dropped to 33±5%, whereas interaction with GS-FeNi–treated TC resulted in enhanced cellular viability of 73±4%.

3.7 Reusability of GS-FeNi

Reusability test was conducted by repeated interaction of already reacted GS-FeNi with fresh TC solution for 4 cycles. The removal efficiency gradually declined with every cycle of reuse (Fig. 8**)** from 1st to 4th cycle. It also indicated that the in situ synthesized nanoparticles were firmly bonded to the sand, suggesting low leach out of the nanoparticles into the aqueous solutions upon reaction with TC.

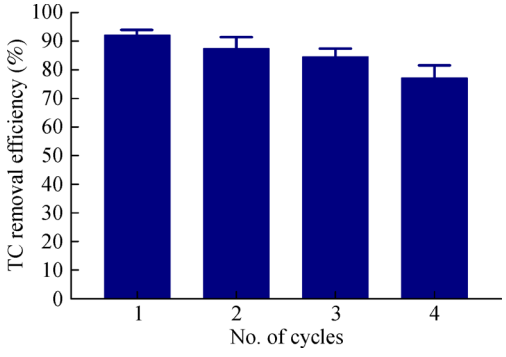

Fig. 8 Reusability of GS-FeNi for further cycles of TC removal.

The elemental Fe and Ni contents in GS-FeNi before and after interaction was estimated, and the data are represented in Table S3A (Supplementary information). From the Table, it can be concluded that after interaction with TC, there was no significant change in the Fe and Ni contents in GS-FeNi. To confirm further, the Fe and Ni ion release was analyzed after all the four cycles of reuse (Table S3B; Supplementary information). The concentration of the leached Fe ions was negligible even after the fourth cycle, while the Ni leaching was below 20 μg/L at the end of the fourth cycle.

The entire sand after stripping out the particles can be reused as fresh sand for the synthesis of the next batch of GS-FeNi. Thus, the sand on which the bimetallic nanoparticles were formed can be reused multiple times, which proves to be a highly economical and environmental friendly approach (Lv et al., 2013).

3.8 Fixed-bed continuous-flow column studies for TC removal

The effect of various flow rates such as 1, 2, and 3 mL/min on TC removal was studied in the column using GS-FeNi, keeping a fixed bed height of 3 cm and TC influent concentration of 20 mg/L. Figure 9A represents that as the flow rate increased, there was a decline in the breakthrough time in the reactor. A decrease in the breakthrough time was observed from 72.1 h to 22 h with a corresponding decrease in the TC removal capacity from 693±7 mg/g to 431±4 mg/g when the flow rate was increased from 1 mL/min to 3 mL/min, respectively. The results can be attributed to the inadequate interaction time between GS-FeNi and TC in the solution with increasing flow rates (Charumathi and Das, 2012; Noreen et al., 2013).

The effect of influent concentration on TC removal is shown in Fig. 9B. The removal capacity decreased from 693±7 mg/g to 398±5 mg/g on increasing the initial TC concentration from 20 mg/L to 60 mg/L at a constant flow rate of 1 mL/min and bed height of 3 cm. As the initial TC concentration was increased from 20 mg/L to 60 mg/L, the exhaustion time for GS-FeNi decreased from 72.1 h to 16.3 h. On increasing the influent TC concentration, the sorbent could have attained the saturated state early (Samuel et al., 2013). The findings corroborate well with the results on removal of phenol from aqueous solution using a fixed-bed column study (Shi et al., 2011).

The effect of varying bed heights was studied by keeping the other experimental conditions constant. The results showed (Fig. 9C) that with increasing bed height (3–10 cm), the breakthrough time increased from 72.1 h to

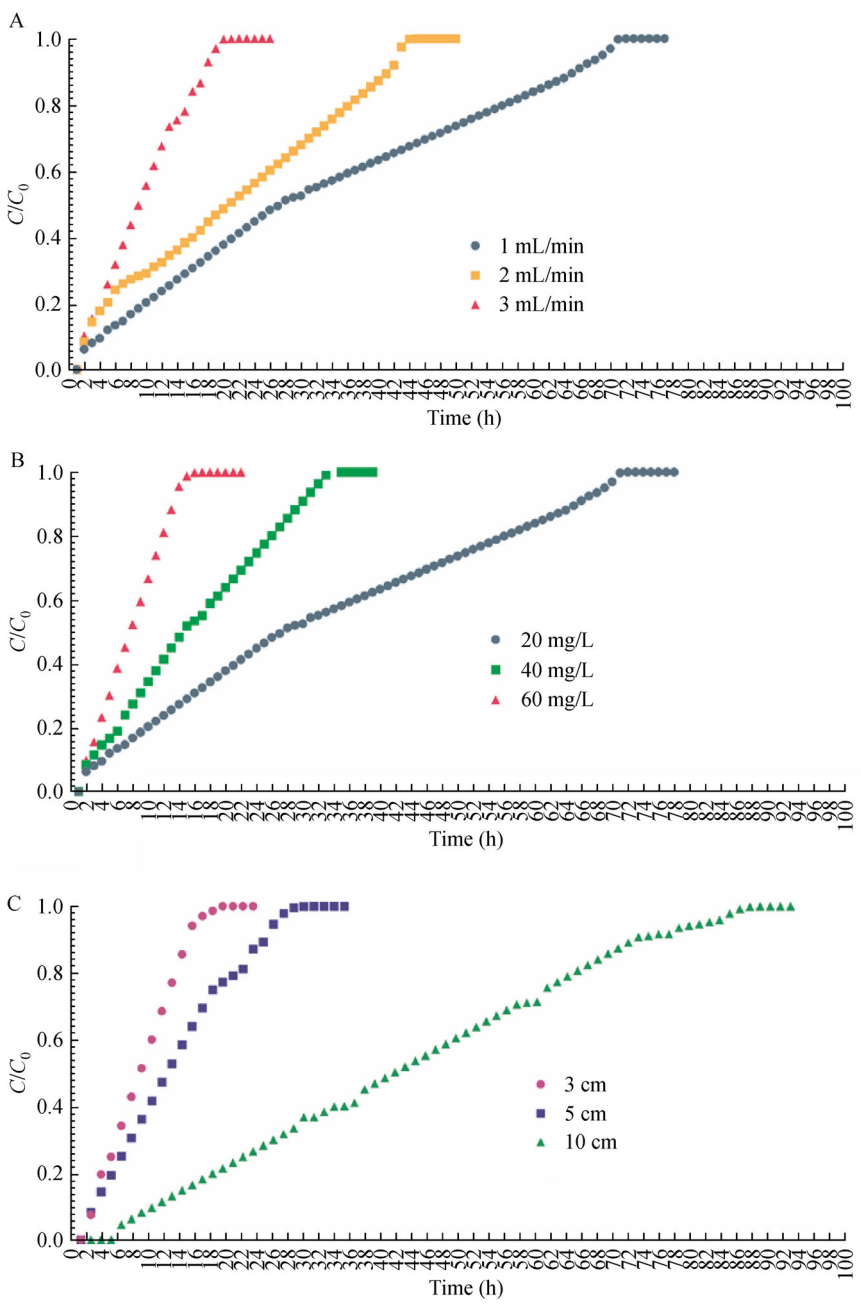

Fig. 9 TC removal using GS-FeNi: Experimental breakthrough curves for (A) different flow rates, (B) different TC initial concentrations, and (C) different bed heights.

339 h with a concomitant increase in the removal capacity from 693±7 mg/g to 978±5 mg/g. It can be clearly inferred that increased bed height resulted in a significant rise in both the breakthrough time and the removal capacity since an increase in the sorbent content of the column resulted in a proportionate increase in the number of reaction sites. These findings correlate quite well with the conclusions from the previous studies (Marzbali and Esmaieli, 2017; Ravikumar et al., 2019a)

Based on the above findings, the optimal operating conditions to remove TC in the column reactor were obtained. With an initial influent TC concentration: 20 mg/L, bed height: 10 cm, and flow rate: 1 mL/min, a maximum TC removal capacity of 978±5 mg/g was noted in GS-FeNi packed column reactor. At time intervals of 1 h and 170 h, the effluent samples were sent for LCMS analysis when the TC removal was 100% and 50%, respectively (Fig. S7, supplementary information). At 1 h, m/z peaks at 288 and 218 were observed, and these products may have formed due to the decarboxylation and break of carboatomic ring B (Hailili et al., 2017; Dong et al., 2018b). In the case of 170-h sample, 345 m/z

(berberine) and 445 m/z were observed. The formation of compound indicated by 345 m/z may be related to the break of carbinol group in C2, while 445 m/z confirmed the presence of TC in the solution (Hailili et al., 2017; Dong et al., 2018b). From the LCMS results, it can be concluded that in the column study also, TC was degraded into smaller organic compounds, which were similar to the batch removal study.

As compared with our previous study (Ravikumar et al., 2019a in Table S1, supplementary information) using chemically-synthesized NiFe-coated sand in column reactor (this was the only study so far regarding TC removal using bimetallic NZVI-coated sand), the removal capacity in the current operation was found to be less; however, the current method has several advantages like one-step green synthesis of the sorbent and avoidance of harsh chemicals like $NaBH_4$.

3.9 Application of GS-FeNi–packed column for real water systems

TC removal by GS-FeNi was validated under optimal conditions using ground water, lake water, and tap water spiked with TC in the packed bed column reactors. The characteristic properties of ground, lake, and tap water are detailed in Table S4 (Supplementary information). Removal capacities of 781±5, 712±5, and 687±3 mg/g were obtained with tap water, ground water, and lake water, respectively. Undeniably, the removal capacity suffered a decline as compared to that of the tests using distilled deionized water in the previous sections. This could happen due to the presence of natural organic components in the real water systems interfering with the process. Previous studies have shown that natural organics in real water system could contribute to the reduced removal capacity of TC using bimetallic nZVI particles (Ravikumar et al., 2016b; Zhang et al., 2017).

4 Conclusions

GS-FeNi was synthesized using simple green synthesis technique. This method is free from any toxic solvents or chemicals for reducing FeNi. The GS-FeNi showed excellent TC removal efficiency in batch and continuous flow reactors. A maximum of 99±0.2% TC removal was obtained in batch study, and the sorbent reusability was proven till the 4th cycle. The mechanism(s) of TC removal involved both sorption on the surface as well as degradation to smaller organics possibly through redox processes. The residual toxicity assays clearly showed that the degradation products of TC were quite less toxic compared with uninteracted TC. Furthermore, interactions in the packed bed continuous reactor using GS-FeNi achieved a very high removal capacity of 978±5 mg/g. The findings suggest a possible means to synthesize a bimetallic nano-sorbent on sand and its effective utilization for TC removal from aqueous solutions. The results from the column reactor studies hold the key to further scaling up the process to treat pharmaceutical pollutants from wastewater. The green composites developed in this work have potential applications in treating other pharmaceuticals also in the near future. Future studies should focus on removing mixed antibiotics or antibiotics mixed with other inorganics or organics to mimic real environmental systems.

Acknowledgements We wholeheartedly thank the Department of Science and Technology-Science and Engineering Research Board (DST-SERB) Organization (Sanction No. EMR/2016/004816) for providing the financial support for carrying out this research work. We would also express sincere gratitude to Dr. Sruthi Ann Alex, Teaching fellow, Centre for Nano Science and Technology, ACTECH- Anna University, Chennai for her help in proof reading the manuscript.

Electronic Supplementary Material Supplementary material is available in the online version of this article at https://doi.org/10.1007/s11783-019-1195-3 and is accessible for authorized users.

References

Ahmad N, Sharma S, Rai R (2012). Rapid green synthesis of silver and gold nanoparticles using peels of Punica granatum. Advanced Materials Letters, 3(5): 376–380

Arivoli S, Dhinamala K, Persis D, Meeran M, Pandeeswari M (2018). Analysis of physicochemical water quality parameters of Buckingham Canal, Chennai, Tamil Nadu, India. International Journal of Zoology Studies, 3(1): 226–231

Blowes DW, Ptacek C J, Jambor J L (1997). In-situ remediation of Cr (VI)-contaminated groundwater using permeable reactive walls: Laboratory studies. Environmental Science & Technology, 31(12): 3348–3357

Charumathi D, Das N (2012). Packed bed column studies for the removal of synthetic dyes from textile wastewater using immobilised dead C. tropicalis. Desalination, 285: 22–30

Chen Y Y, Ma Y L, Yang J, Wang L Q, Lv J M, Ren C J (2017). Aqueous tetracycline degradation by H_2O_2 alone: Removal and transformation pathway. Chemical Engineering Journal, 307: 15–23

Dai Y J, Liu M, Li J J, Yang S S, Sun Y, Sun Q Y, Wang W S, Lu L, Zhang K X, Xu J Y, Zheng W L, Hu Z Y, Yang Y H, Gao Y W, Liu Z H (2019). A review on pollution situation and treatment methods of tetracycline in groundwater. Separation Science and Technology, 6395: 1–17

Danner M C, Robertson A, Behrends V, Reiss J (2019). Antibiotic pollution in surface fresh waters: Occurrence and effects. Science of the Total Environment, 664 (2019): 793–804

Dong H, Jiang Z, Deng J, Zhang C, Cheng Y, Hou K, Zhang L, Tang L, Zeng G (2018a). Physicochemical transformation of Fe/Ni bimetallic nanoparticles during aging in simulated groundwater and the consequent effect on contaminant removal. Water Research, 129: 51–57

Dong H, Jiang Z, Zhang C, Deng J, Hou K, Cheng Y, Zhang L, Zeng G

(2018b). Removal of tetracycline by Fe/Ni bimetallic nanoparticles in aqueous solution. Journal of Colloid and Interface Science, 513: 117–125

Du L, Luo L L, Feng Z X, Engelhard M, Xie X H, Han B H, Sun J M, Zhang J H, Yin G P, Wang C M, Wang Y, Shao Y Y (2017). Nitrogen–doped graphitized carbon shell encapsulated NiFe nanoparticles: A highly durable oxygen evolution catalyst. Nano Energy, 39: 245–252

Fowkes F M, Anderson F W, Berger J E (1970). Bimetallic coalescers: Electrophoretic coalescence of emulsions in beds of mixed-metal granules. Environmental Science & Technology, 4(6): 510–514

Fu F, Ma J, Xie L, Tang B, Han W, Lin S (2013). Chromium removal using resin supported nanoscale zero-valent iron. Journal of Environmental Management, 128: 822–827

Gheju M, Balcu I, Mosoarca G (2016). Removal of Cr(VI) from aqueous solutions by adsorption on MnO_2. Journal of Hazardous Materials, 310: 270–277

Gokhale S V, Jyoti K K, Lele S S (2009). Modeling of chromium(VI) biosorption by immobilized *Spirulina platensis* in packed column. Journal of Hazardous Materials, 170(2-3): 735–743

Gottschall N, Topp E, Metcalfe C, Edwards M, Payne M, Kleywegt S, Russell P, Lapen D R (2012). Pharmaceutical and personal care products in groundwater, subsurface drainage, soil, and wheat grain, following a high single application of municipal biosolids to a field. Chemosphere, 87(2): 194–203

Hailili R, Wang Z Q, Xu M, Wang Y, Gong X Q, Xu T, Wang C (2017). Layered nanostructured ferroelectric perovskite $Bi_5FeTi_3O_{15}$ for visible light photodegradation of antibiotics. Journal of Materials Chemistry. A, Materials for Energy and Sustainability, 5(40): 21275–21290

Huang B, Liu Y, Li B, Liu S, Zeng G, Zeng Z, Wang X, Ning Q, Zheng B, Yang C (2017). Effect of Cu(II) ions on the enhancement of tetracycline adsorption by Fe_3O_4@SiO_2-Chitosan/graphene oxide nanocomposite. Carbohydrate Polymers, 157: 576–585

Jiang X, Guo Y, Zhang L, Jiang W, Xie R (2018). Catalytic degradation of tetracycline hydrochloride by persulfate activated with nano Fe^0 immobilized mesoporous carbon. Chemical Engineering Journal, 341: 392–401

Jin X Y, Liu Y, Tan J, Owens G, Chen Z L (2018). Removal of Cr(VI) from aqueous solutions via reduction and absorption by green synthesized iron nanoparticles. Journal of Cleaner Production, 176: 929–936

Kadu B S, Wani K D, Kaul-Ghanekar R, Chikate R C (2017). Degradation of doxorubicin to non-toxic metabolites using Fe-Ni bimetallic nanoparticles. Chemical Engineering Journal, 325: 715–724

Kang J, Liu H, Zheng Y M, Qu J, Chen J P (2010). Systematic study of synergistic and antagonistic effects on adsorption of tetracycline and copper onto a chitosan. Journal of Colloid and Interface Science, 344 (1): 117–125

Kango, Kumar (2016). Magnetite nanoparticles coated sand for arsenic removal from drinking water. Environmental Earth Sciences, 75(5): 1-12

Kaviya S (2017). Rapid naked eye detection of arginine by pomegranate peel extract stabilized gold nanoparticles. Journal of King Saud University-Science, 29(4), 436–443

Li Y, Guo C, Yang J, Wei J, Xu J, Cheng S (2006). Evaluation of antioxidant properties of pomegranate peel extract in comparison with pomegranate pulp extract. Food Chemistry, 96(2): 254–260

Li Z J, Wang L, Yuan L Y, Xiao C L, Mei L, Zheng L R, Zhang J, Yang J H, Zhao Y L, Zhu Z T, Chai Z F, Shi W Q (2015). Efficient removal of uranium from aqueous solution by zero-valent iron nanoparticle and its graphene composite. Journal of Hazardous Materials, 290: 26–33

Lv X, Jiang G, Xue X, Wu D, Sheng T, Sun C, Xu X (2013). Fe^0-Fe_3O_4 nanocomposites embedded polyvinyl alcohol/sodium alginate beads for chromium (VI) removal. Journal of Hazardous Materials, 262: 748–758

Ma K, Wang Q, Rong Q, Zhang D, Cui S, Yang J (2017). Preparation of magnetic carbon/Fe_3O_4 supported zero-valent iron composites and their application in Pb(II) removal from aqueous solutions. Water Sci Technol, 76(10): 2680–2689

Marzbali M H, Esmaieli M (2017). Fixed bed adsorption of tetracycline on a mesoporous activated carbon: Experimental study and neuro-fuzzy modeling. Journal of Applied Research and Technology, 15(5): 454–463

Marzo A, Dal Bo L (1998). Chromatography as an analytical tool for selected antibiotic classes: a reappraisal addressed to pharmacokinetic applications. Journal of Chromatography. A, 812(1-2): 17–34

Miao X S, Bishay F, Chen M, Metcalfe C D (2004). Occurrence of antimicrobials in the final effluents of wastewater treatment plants in Canada. Environmental Science & Technology, 38(13): 3533–3541

Natarajan S, Bhuvaneshwari M, Lakshmi D S, Mrudula P, Chandrasekaran N, Mukherjee A (2016). Antibacterial and antifouling activities of chitosan/TiO_2/Ag NPs nanocomposite films against packaged drinking water bacterial isolates. Environmental Science and Pollution Research International, 23(19): 19529–19540

Noreen, Bhatti, Nausheen, Sadaf, Ashfaq (2013). Batch and fixed bed adsorption study for the removal of Drimarine Black CL-B dye from aqueous solution using a lignocellulosic waste: A cost affective adsorbent. Industrial Crops and Products, 50: 568–579

Oladoja, Aboluwoye, Oladimeji (2009). Kinetics and isotherm studies on methylene blue adsorption onto ground palm kernel coat. Turkish Journal of Engineering and Environmental Sciences, 32(5): 303–312

Öztürk, Malkoc (2014). Adsorptive potential of cationic Basic Yellow 2 (BY2) dye onto natural untreated clay (NUC) from aqueous phase: Mass transfer analysis, kinetic and equilibrium profile. Applied Surface Science, 299: 105–115

Pulugandi C (2014). Analysis of water quality parameters in Vembakottai water reservoir, Virudhunagar district, Tamil Nadu-a report. Research Journal of Recent Sciences, 3(ISC-2013)): 242–247

Punamiya P, Sarkar D, Rakshit S, Datta R (2015). Effect of solution properties, competing ligands, and complexing metal on sorption of tetracyclines on Al-based drinking water treatment residuals. Environmental Science and Pollution Research International, 22 (10): 7508–7518

Qiu B, Xu C X, Sun D Z, Wei H G, Zhang X, Guo J, Wang Q, Rutman D, Guo Z H, Wei S Y (2014). Polyaniline coating on carbon fiber fabrics for improved hexavalent chromium removal. RSC Advances, 4(56): 29855–29865

Ravikumar, Kumar, Kumar, Mrudula, Natarajan, Mukherjee (2016a). Enhanced Cr(VI) removal by nanozerovalent iron-immobilized

alginate beads in the presence of a biofilm in a continuous-flow reactor. Industrial & Engineering Chemistry Research, 55(20): 5973–5982

Ravikumar, Sudakaran, Ravichandran, Pulimi, Natarajan, Mukherjee (2019b). Green synthesis of NiFe nano particles using *Punica granatum* peel extract for tetracycline removal. Journal of Cleaner Production, 210: 767–776

Ravikumar K V, Kumar D, Rajeshwari A, Madhu G M, Mrudula P, Chandrasekaran N, Mukherjee A (2016b). A comparative study with biologically and chemically synthesized nZVI: Applications in Cr (VI) removal and ecotoxicity assessment using indigenous micro-organisms from chromium-contaminated site. Environmental Science and Pollution Research International, 23(3): 2613–2627

Ravikumar K V G, Singh A S, Sikarwar D, Gopal G, Das B, Mrudula P, Natarajan C, Mukherjee A (2019a). Enhanced tetracycline removal by in-situ NiFe nanoparticles coated sand in column reactor. Journal of Environmental Management, 236: 93–99

Roy B, Chandrasekaran H, Palamadai Krishnan S, Chandrasekaran N, Mukherjee A (2018). UV pre-irradiation to P25 titanium dioxide nanoparticles enhanced its toxicity towards freshwater algae Scenedesmus obliquus. Environmental Science and Pollution Research International, 25(17): 16729–16742

Samuel J, Pulimi M, Paul M L, Maurya A, Chandrasekaran N, Mukherjee A (2013). Batch and continuous flow studies of adsorptive removal of Cr(VI) by adapted bacterial consortia immobilized in alginate beads. Bioresource Technology, 128: 423–430

Shao Y, Gao Y, Yue Q, Kong W, Gao B, Wang W, Jiang W (2020). Degradation of chlortetracycline with simultaneous removal of copper (II) from aqueous solution using wheat straw-supported nanoscale zero-valent iron. Chemical Engineering Journal, 379: 122384

Shi L N, Zhang X, Chen Z L (2011). Removal of chromium (VI) from wastewater using bentonite-supported nanoscale zero-valent iron. Water Research, 45(2): 886–892

Song Z, Ma Y L, Li C E (2019). The residual tetracycline in pharmaceutical wastewater was effectively removed by using MnO_2/graphene nanocomposite. Science of the Total Environment, 651(Pt 1): 580–590

Tabrizian P, Ma W, Bakr A, Rahaman M S (2019). pH-sensitive and magnetically separable Fe/Cu bimetallic nanoparticles supported by graphene oxide (GO) for high-efficiency removal of tetracyclines. Journal of Colloid and Interface Science, 534: 549–562

Tang L, Yang G D, Zeng G M, Cai Y, Li S S, Zhou Y Y, Pang Y, Liu Y Y, Zhang Y, Luna B (2014). Synergistic effect of iron doped ordered mesoporous carbon on adsorption-coupled reduction of hexavalent chromium and the relative mechanism study. Chemical Engineering Journal, 239: 114–122

Turku I, Sainio T, Paatero E (2007). Thermodynamics of tetracycline adsorption on silica. Environmental Chemistry Letters, 5(4): 225–228

Vijayakumar N S, Flower N A L, Brabu B, Gopalakrishnan C, Raja S V K (2013). Degradation of DCE and TCE by Fe–Ni nanoparticles immobilised polysulphone matrix. Journal of Experimental Nanoscience, 8(7-8): 890–900

Weng X L, Cai W L, Lan R F, Sun Q, Chen Z L (2018). Simultaneous removal of amoxicillin, ampicillin and penicillin by clay supported Fe/Ni bimetallic nanoparticles. Environmental Pollution, 236: 562–569

Wu Y, Yue Q, Gao Y, Ren Z, Gao B (2018). Performance of bimetallic nanoscale zero-valent iron particles for removal of oxytetracycline. Journal of Environmental Sciences (China), 69: 173–182

Xiong W P, Zeng G M, Yang Z H, Zhou Y Y, Zhang C, Cheng M, Liu Y, Hu L, Wan J, Zhou C Y, Xu R, Li X (2018). Adsorption of tetracycline antibiotics from aqueous solutions on nanocomposite multi-walled carbon nanotube functionalized MIL-53(Fe) as new adsorbent. Science of the Total Environment, 627: 235–244

Yan M, Wu Y L, Zhu F F, Hua Y Q, Shi W D (2016). The fabrication of a novel Ag_3VO_4/WO_3 heterojunction with enhanced visible light efficiency in the photocatalytic degradation of TC. Phys Chem Chem Phys, 18(4): 3308–3315

Yue Z, Bender S E, Wang J, Economy J (2009). Removal of chromium Cr(VI) by low-cost chemically activated carbon materials from water. Journal of Hazardous Materials, 166(1): 74–78

Zhang Y, Jiao Z, Hu Y, Lv S, Fan H, Zeng Y, Hu J, Wang M (2017). Removal of tetracycline and oxytetracycline from water by magnetic Fe_3O_4@graphene. Environmental Science and Pollution Research International, 24(3): 2987–2995

Zhou Y Z, Wang T, Zhi D, Guo B L, Zhou Y Y, Nie J, Huang A Q, Yang Y, Huang H L, Luo L (2019). Applications of nanoscale zero-valent iron and its composites to the removal of antibiotics: A review. Journal of Materials Science, 54(19): 12171–12188